

Doubly Helical Coronal Ejections from Dynamos and their Role in Sustaining the Solar Cycle

Eric G. Blackman¹ & Axel Brandenburg²

1. *Department of Physics & Astronomy, and Laboratory for Laser Energetics, University of Rochester, Rochester NY 14627*

2. *Nordita, Blegdamsvej 17, DK-2100 Copenhagen Ø, Denmark*

ABSTRACT

Two questions about the solar magnetic field might be answered together once their connection is identified. The first is important for large scale dynamo theory: what prevents the magnetic backreaction forces from shutting down the dynamo cycle? The second question is: what determines the handedness of twist and writhe in magnetized coronal ejecta? Magnetic helicity conservation is important for answering both questions. Conservation implies that dynamo generation of large scale writhed structures is accompanied by the oppositely signed twist along these structures. The latter is associated with the backreaction force. We suggest that coronal mass ejections (CMEs) simultaneously liberate small scale twist and large scale writhe of opposite sign, helping to prevent the cycle from quenching and enabling a net magnetic flux change in each hemisphere. Observations and helicity spectrum measurements from a numerical simulation of a rising flux ribbon in the presence of rotation support this idea. We show a new pictorial of dynamo flux generation that includes the backreaction and magnetic helicity conservation by characterizing the field as a 2-D ribbon rather than a 1-D line.

Subject Headings: MHD–Sun: activity–Sun: magnetic fields MHD–turbulence; stars–magnetic fields; galaxies–magnetic fields; methods–numerical

1. Introduction

The helical magnetic dynamo is the basis for a promising class of mechanisms to explain large scale magnetic fields observed in stars and galaxies (Parker 1974; Moffatt 1978; Krause & Rädler 1980; Parker 1993). The basic “ $\alpha - \Omega$ ” dynamo is the specific version most relevant for strongly sheared rotators (Fig. 1). Interface $\alpha - \Omega$ dynamos (Parker 1993;

Charbonneau & MacGregor 1996; Markiel & Thomas 1999) include the fact that, unlike for galaxies and disks, the dominant shear layer is beneath the dominant turbulent region.

Focusing on the simplest “ $\alpha - \Omega$ ” picture (Fig. 1), consider an initially weak toroidal (=encircling the rotation axis) loop of the magnetic field embedded in the astrophysical plasma rotator. The magnetic field is coupled to the plasma so the field is carried or stretched in response to the plasma motion. Now imagine, as in the sun, that there is an outwardly decreasing density gradient. Consider the motion of a rising turbulent swirl of gas, threaded by a magnetic field. Conservation of angular momentum dictates that the swirl will writhe oppositely to the underlying rotation of the system. This means that the initially toroidal field threading the swirl gains a radial component. Statistically, rising swirls in the northern (southern) hemisphere writhe the field clockwise (counterclockwise). This is the “ α ” effect and is shown by the writhed loop of Fig. 1a for the northern hemisphere. Differential rotation at the base of the loop shears the radial field (the “ Ω ”-effect). The bottom part of the loop amplifies the initial toroidal seed loop as shown in Fig. 1b, whilst the top part of the loop diffuses away (the “ β ” effect). In doing so, magnetic flux is amplified: the flux penetrating the tilted rectangular surface is zero in Fig. 1a, but finite in Fig. 1b.

This process is represented mathematically by averaging the magnetic induction equation over a local volume and breaking all quantities (velocity \mathbf{U} , magnetic field \mathbf{B} in Alfvén velocity units, and normalized current density $\mathbf{J} \equiv \nabla \times \mathbf{B}$) into their mean (indicated by an overbar) and fluctuating (indicated by lower case) components. The result is (Moffatt 1978): $\partial_t \overline{\mathbf{B}} = \nabla \times (\alpha \overline{\mathbf{B}} + \overline{\mathbf{U}} \times \overline{\mathbf{B}}) + (\beta + \lambda) \nabla^2 \overline{\mathbf{B}}$, where λ is the microphysical diffusivity. The $\overline{\mathbf{U}}$ term incorporates the Ω -effect, the β term incorporates the turbulent diffusion (assuming constant β) and the first term on the right incorporates the α -effect. In the kinematic theory (Moffatt 1978) α is given by $\alpha = \alpha_0 = -(\tau/3) \overline{\mathbf{u} \cdot \nabla \times \mathbf{u}}$. Here τ is a turbulent damping time and $\overline{\mathbf{u} \cdot \nabla \times \mathbf{u}}$ is the kinetic helicity, which dictates the α -effect described physically above. Usually, α and β are prescribed as input parameters.

A long standing problem has been the absence of properly incorporating the (time-dependent) backreaction from the growing magnetic field on the driving turbulent motions. This stimulated criticisms of mean-field dynamos (Piddington 1981; Cattaneo & Hughes 1996) and motivated interface dynamo models (Parker 1993). But the backreaction is now much better understood. Steady-state studies of α -quenching (Cattaneo & Hughes 1996) apply only at fully saturated dynamo regimes, not at early times, when the backreaction is just beginning to be important. There the growth is fast, and most relevant for astrophysics. Demonstrating this requires including the time-evolution of the turbulent velocity, subject to magnetic forces. Carrying this out formally (Blackman & Field 2002) and using a closure in which triple correlations act as a damping term, amounts to replacing $\alpha = \alpha_0$

by $\alpha = \alpha_0 + (\tau/3)\overline{\mathbf{b} \cdot \nabla \times \mathbf{b}}$, where the second term is the backreaction. It arises from $(\nabla \times \mathbf{b}) \times \overline{\mathbf{B}}$, the force associated with the action of the small scale current and the large scale field. This residual form of α has long been thought (Pouquet et al. 1976) to be the real driver of the helical dynamo and has been employed in attempts to understand its quenching (Zeldovich et al. 1983; Kleeorin & Ruzmaikin 2002; Field & Blackman 2002; Blackman & Brandenburg 2002) From the form of α , it is evident that a large current helicity can offset the kinetic helicity and quench the dynamo (Field & Blackman 2002; Blackman & Brandenburg 2002).

In section 2 we summarize the successful backreaction theory, and show how it predicts ejection of twist and writhe of opposite sign. In section 3 we give a new pictorial of dynamo action that includes magnetic helicity conservation, and discuss a simulation of a rising flux ribbon. Observational implications are discussed in section 4, and we conclude in section 5.

2. Role of Magnetic Helicity Conservation

The principle of magnetic helicity conservation determines the strength of the current helicity correction term in α discussed in the previous section. The magnetic helicity, defined by a volume integral $H \equiv \int \mathbf{A} \cdot \mathbf{B} dV \equiv \langle \mathbf{A} \cdot \mathbf{B} \rangle V$, satisfies (Woltjer 1958; Berger & Field 1984)

$$\partial_t H = -2\lambda C - \text{surface terms}, \quad (1)$$

where the magnetic field \mathbf{B} is related to \mathbf{A} by $\mathbf{B} = \nabla \times \mathbf{A}$, and the current helicity C is defined by $C \equiv \langle \mathbf{J} \cdot \mathbf{B} \rangle V$. Without the surface terms (which represent flow through boundaries) H is well conserved: for $\lambda \rightarrow 0$ the λ term in (1) converges to zero (Berger 1984).

The magnetic helicity is a measure of “linkage” and “twist” of field lines (Berger & Field 1984). Equation (1) then means that in a closed system, the total amount of twist and writhe is conserved. If the large scale field is writhed one way, then the small scale field must twist oppositely. In the sun, differential rotation and cyclonic convection (the α -effect) are both sources of helicity, (Berger & Ruzmaikin 2000; DeVore 2000) but here we focus on the α -effect, which generates large scale poloidal structures.

The α -effect does not produce a net magnetic twist but produces simultaneously positive and negative magnetic twists on different scales (Seehafer 1996; Ji 1999; Blackman & Field 2000; Brandenburg 2001; Field & Blackman 2002). The importance of this scale segregation of H for the backreaction term in α is easily seen in the two-scale approach. Here we write $H = H_1 + H_2$, where $H_1 = \langle \overline{\mathbf{A}} \cdot \overline{\mathbf{B}} \rangle V$ and $H_2 = \langle \overline{\mathbf{a}} \cdot \overline{\mathbf{b}} \rangle V$ correspond to the volume integrated large and small scale contributions respectively. For C , we then have $C = \langle \overline{\mathbf{J}} \cdot \overline{\mathbf{B}} \rangle V + \langle \overline{\mathbf{j}} \cdot \overline{\mathbf{b}} \rangle V = k_1^2 H_1 + k_2^2 H_2$, where k_1 and k_2 represent the wavenumbers (inverse gradients) associated with

the large and small scales respectively, and the second equality follows rigorously for a closed system. The current helicity backreaction in $\langle \alpha \rangle$ is thus $k_2^2 H_2$.

We now relate $\overline{\mathbf{B}}$ to H_1 . We define ϵ_1 such that the large scale magnetic energy $\langle \overline{\mathbf{B}}^2 \rangle V = H_1 k_1 / \epsilon_1$ and where $0 < |\epsilon_1| \leq 1$, where $|\epsilon_1| = 1$ only for a force-free helical large scale field (i.e. for which $\overline{\mathbf{J}} \parallel \overline{\mathbf{B}}$ so that the force $\overline{\mathbf{J}} \times \overline{\mathbf{B}} = 0$). In the northern hemisphere $\epsilon_1 > 0$. By writing conservation equations analogous to (1) for H_1 and H_2 respectively, we obtain

$$\partial_t H_1 = 2S - 2\lambda k_1^2 H_1 - \text{surface terms} \quad (2)$$

and

$$\partial_t H_2 = -2S - 2\lambda k_2^2 H_2 - \text{surface terms} \quad (3)$$

where we have used $S = (\langle \alpha \rangle k_1 / \epsilon_1 - \langle \beta \rangle k_1^2) H_1$ and $\langle \alpha \rangle = (\langle \alpha_0 \rangle + \frac{1}{3} \tau k_2^2 H_2 / V)$. The case without surface terms and with $\epsilon_1 = 1$ represents a dynamo without differential rotation. The solution (Field & Blackman 2002; Blackman & Brandenburg 2002; Blackman & Field 2002) shows that for initially small H_2 but large α_0 , H_1 grows. Growth of H_1 implies the oppositely signed growth of H_2 . This H_2 backreacts on α_0 , ultimately quenching $\langle \alpha \rangle$ and the dynamo.

Since the sun is a differentially rotating open system, differential rotation and surface terms are important. The former forces $|\epsilon_1| < 1$, and ϵ_1 a function of time to reflect the solar cycle. The presence of surface terms generally requires the use of the relative magnetic helicity (Berger & Field 1984) but to capture the key points, we can instead treat them as diffusion terms (1). We combine the λ and surface terms of both (2) and (3) into the forms $-\nu_1 k_1^2 H_1$ and $-\nu_2 k_2^2 H_2$ respectively. We consider the volume average $\langle \rangle$ to be taken over one hemisphere and assume that surface terms represent diffusion into the corona. On time scales much shorter than the 11 year solar half cycle, the left sides of (2) and (3) are negligible and the system is in a relatively steady state. We then see that the boundary terms are equal and opposite (Blackman & Field 2000). Here this implies $\nu_1 k_1^2 |H_1| \simeq \nu_2 k_2^2 |H_2|$. Since the boundary diffusion terms represent a flux of (relative) magnetic helicity to the exterior, these quantities are connected to measurable observables. *We therefore predict that the shedding rates of small scale twist and large scale writhe from the α effect are equal in magnitude and opposite in sign.*

3. Revising the “Textbook” Dynamo Pictorial

The helicity conservation, shedding, and magnetic backreaction are represented simply in Figs. 1c–e for the northern hemisphere. The key is representing the field by a two-dimensional ribbon instead of a one-dimensional line.

Comparing Figs. 1a & b (H conservation not included) with Figs. 1c & d (H conservation included) we see that in the latter, as the α -effect produces its large scale writhe (the loop corresponding to gradient scale k_1^{-1}) it also twists the ribbon (corresponding to gradient scale k_2^{-1}). The large-scale writhe is right handed, but the twist along the ribbon is left-handed and so the total H is conserved. This is the simplest generalization of the picture in Fig. 1a, to include helicity conservation. The ribbon should be thought of as a mean field, averaged over smaller fluctuations, and so the actual field need not be so smooth.

The top view is shown in Fig. 1e for comparison to observations. In the northern hemisphere we expect an N shaped (or reverse-S) sigmoid prominence and in the southern hemisphere we would expect an S shaped sigmoid. In Fig. 1e we also show the backreaction force corresponding to the small-scale magnetic twist along the ribbon: it fights against writhing or bending the ribbon. Eventually this twisting would suppress the α effect (and thus statistically, its hemispheric average $\langle\alpha\rangle$ entering (2) and (3)), which thrives on being able to writhe the ribbon. In the sun, such sigmoid structures precede CMEs (Pevtsov & Canfield 1999) which on time scales of order days or weeks dissipate both the writhe and twist. In doing so, they help alleviate the backreaction on the α effect, and allow a net amplification of magnetic flux inside the sun as shown in Fig. 1c. Some loops produced by the dynamo may not escape, implying that some of the simultaneous diffusion of H_1 and H_2 is hidden in the solar interior. But even so, the helicity fluxes of H_1 and H_2 from the loops which do escape, should still be equal and opposite. Getting rid of H_2 simultaneously with H_1 , either internally or externally, is what alleviates the backreaction, external removal by means of CMEs is one important aspect of how this occurs. Removal of H_2 implies that by solar minimum the α effect is again driven by α_0 , allowing the cycle to repeat.

We have performed a numerical simulation to measure the magnetic helicity spectrum of a buoyant magnetic flux ribbon in the presence of rotation which confirms the basic ideas that twist and writhe emerge with opposite sign. Though rising flux tube simulations have been carried out in the past (Abbett et al. 2000) they have not focused on the magnetic helicity spectrum. We started with a toroidal, horizontal flux tube and a vertically dependent sinusoidal modulation of the entropy along the ribbon. This destabilizes the ribbon to buckle and rise in one portion. The boundaries were sufficiently far away to use a Fourier transform to obtain power spectra (Fig. 2). After 6 free-fall times the spectrum shows mostly positive magnetic helicity together with a gradually increasing higher wavenumber component of negative spectral helicity density. The latter is the anticipated contribution from the twist along the ribbon.

4. Observational Implications

In comparing the above results with observations note that the magnetic helicity is a volume integral, so the ribbon on which the twisted prominence arises may have a hidden twist elsewhere inside the sun. This subtlety is surmounted by use of the relative magnetic helicity (Berger & Field 1984) which allows a quantifiable interpretation of locally twisted structures. Observations typically measure the current helicity density, $\mathbf{J} \cdot \mathbf{B}$, within a single structure, from which hemispheric averages can be computed, or the surface-integrated relative magnetic helicity fluxes.

Existing observations seem to be consistent with our basic picture. First, the observed **N** sigmoids outnumber **S** sigmoids by a ratio of 6:1 in the northern hemisphere with the expected reverse relation in the southern hemisphere (Rust & Kumar 1996). Studies of sigmoids such as Gibson et al. 2002 and refs. therein) do seem to show qualitative agreement with our picture. Figure 2a of Gibson et al. (2002) shows a TRACE image of an **N**-sigmoid (right-handed writhe) with left-handed twisted filament of the active region NOAA AR 8668, typical of the northern hemisphere just as we predict. (As our theory is statistical in nature, it is also not surprising that occasionally **N** sigmoids such as AR8100 (as opposed to **S** sigmoids) appear in the southern hemisphere (Green et al. 2002). But even for AR8100, the writhe is opposite in sign to the twist along the prominence.) Second, recent work confirms a basic hemispheric dependence of the sign of small scale current helicity, corresponding to the twist along the ribbon in Fig. 1c. Measurements of small scale current helicity densities and surface-integrated relative magnetic helicity fluxes (Chae 2000; Berger & Ruzmaikin 2000) as well as fits to line of sight magnetograms of solar active regions (Seehafer 1990; Rust & Kumar 1996; Bao et al. 1999; Pevtsov & Latushko 2000) show primarily negative values in the north and positive in the south. These studies measure the sign of the twist along the ribbon not the writhe of the ribbon itself. We therefore agree that signs of current helicity measured by these line of sight magnetograms are characteristic of the small scale rather than the large scale field (Rädler & Seehafer 1990). Twist is expected at the apex of a writhed prominence since the density is lowest (Parker 1974; Choudhuri 2002).

In sum, Fig. 1e, showing an **N** sigmoid is consistent with the dominant structures of the northern hemisphere. Large scale positive writhe dominates in the north, and large scale negative writhe dominates in the south. Small scale twists along the prominences are predominately negative in the north and positive in the south, so as to produce a very small net helicity in each hemisphere. This is complementary to Demoulin et. al (2002) where oppositely signed twist and writhe from shear were shown to be able to largely cancel, producing a small total magnetic helicity. Here we focused on the α -effect which has the same effect. Finally note that our $\overline{\mathbf{B}}$ represents a local averaging over the small scale twist

so that $\overline{\mathbf{B}}$ has only the writhe (Fig. 1a is thus applicable to $\overline{\mathbf{B}}$, whereas Fig 1c shows both $\overline{\mathbf{B}}$ and \mathbf{b}). On even larger scales, the globally averaged field computed by an azimuthal average $\langle \overline{\mathbf{B}}_\phi \rangle$, is weaker than $\overline{\mathbf{B}}_\phi$ in a local structure, due to the small filling fraction.

5. Conclusion

We have suggested that a new understanding of how helical dynamos conserve magnetic helicity may help resolve several mysteries of the solar magnetic field. We have shown that large and small scale helicities of approximately equal magnitude should be ejected into the solar corona as part of the sustenance of the solar cycle. The large scale helicity corresponds to the writhe of a prominence, whilst the small scale helicity corresponds to the twist along the prominence. We emphasize the importance of simultaneously detecting large and small scale contributions to the losses of helical magnetic fields in pre-CME sigmoid structures at the solar surface. The observations seem to be roughly consistent with our simple picture at present but more studies and detailed modeling will be needed to test these ideas. Our Fig. 1 illustrates the basic concepts through a new pictorial representation of the mean field dynamo that includes magnetic helicity conservation and the backreaction. The implications are also relevant for large scale dynamos in other stars and disks in astrophysics.

EB acknowledges DOE grant DE-FG02-00ER54600, and the Dept. of Astrophys. Sciences at Princeton for hospitality during a sabbatical. We acknowledge PPARC supported supercomputers at Leicester and St Andrews, and the Odense Beowulf cluster is acknowledged.

REFERENCES

- Abbett, W. P., Fisher, G. H., & Fan, Y. 2000, ApJ, 540, 548
- Bao, S. D., Zhang, H. Q., Ai, G. X., & Zhang, M. 1999 A&A, 139, 311
- Berger, M. A. 1984, Geophys. Astrophys. Fluid Dyn., 30, 79
- Berger, M., & Field, G. B. 1984, J. Fluid Mech., 147, 133
- Berger, M. A., & Ruzmaikin, A. 2000, J. Geophys. Res., 105, 10481
- Bhattacharjee A. & Yuan, Y. 1995, ApJ, 449, 739
- Blackman, E.G. 2002 to appear in *Turbulence and Magnetic Fields in Astrophysics* eds. E. Falgarone and T. Passot, Springer Lecture Notes in Physics (astro-ph/0205002)

- Blackman, E.G., & Brandenburg, A. 2002, ApJ, 579, 359
- Blackman, E. G. & Field, G. B. 2000, MNRAS, 318, 724
- Blackman, E.G., & Field, G.B. 2002, Phys. Rev. Lett., in press.
- Brandenburg, A. 2001 ApJ, 550, 824
- Brandenburg, A. 2002 to appear in *Turbulence and Magnetic Fields in Astrophysics*, eds. E. Falgarone and T. Passot, Springer Lecture Notes in Physics (astro-ph/0207394)
- Brandenburg, A., Dobler, W., & Subramanian, K. 2002, Astron. Nach., 323, 99
- Cattaneo, F., & Hughes D.W. 1996, Phys Rev. E., 54, 4532
- Chae, J. 2000, ApJ, 540, L115
- Charbonneau, P., & MacGregor, K. B. 1996, ApJL, 473, L59
- Choudhuri A.R., 2002, astro-ph/0211591.
- Démoulin, P., Mandrini, C. H., Van Driel-Gesztelyi, L., Lopez Fuentes, M. C., & Aulanier, G. 2002, Solar Phys., 207, 87
- Démoulin, P., Mandrini, C. H., van Driel-Gesztelyi, L., Thompson, B. J., Plunkett, S., Kovári, Z., Aulanier, G., & Young, A. 2002, A.& Ap., 382, 650
- DeVore, C. R. 2000, ApJ, 539, 944
- Field, G.B., & Blackman, E.G. 2002, ApJ, 572, 685
- Field, G.B., Blackman E.G., & Chou, H. 1999, ApJ, 513, 638
- Gibson, S. E. et al. 2002, ApJ, 574, 1021
- Green, L. M., López fuentes, M. C., Mandrini, C. H., Démoulin, P., Van Driel-Gesztelyi, L., & Culhane, J. L. 2002, Solar. Phys., 208, 43
- Gruzinov A.V. & Diamond P.H. 1994, Phys. Rev. Lett., 72, 1651
- Ji, H. 1999, Phys. Rev. Lett., 83, 3198
- Kleeorin, N.I., & Ruzmaikin, A.A. 1982, Magnetohydrodynamics, 18, 116
- Kleeorin N., Rogachevskii, I., & Ruzmaikin A. 1995, A&A, 297, L59

- Krause, F., & Rädler, K.-H. 1980, *Mean-Field Magnetohydrodynamics and Dynamo Theory* (Akademie-Verlag, Berlin; also Pergamon Press, Oxford)
- Markiel, J. A. & Thomas, J. H. 1999, *ApJ*, 523, 827
- Moffatt, H. K., *Magnetic Field Generation in Electrically Conducting Fluids*, (Cambridge University Press, Cambridge 1978)
- Piddington, J.H., *Cosmical Electrodynamics*, (Krieger Press, Malabar, 1981)
- Parker, E.N. 1955, *ApJ*, 122, 293
- Parker, E.N. 1974, *ApJ*, 191, 245
- Parker, E.N. 1993, *ApJ*, 408, 707
- Pevtsov, A. A., & Canfield, R. C. 1999, *Geophys. Monographs*, 111, 103
- Pevtsov, A. A. & Latushko, S. M. 2000, *ApJ*, 528, 999
- Pouquet, A., Frisch, U., & Leorat, J. 1976, *J. Fluid Mech.*, 77, 321
- Rädler, K.-H., & Seehafer, N., 1990 in *Topological Fluid Mechanics*, H. K. Moffatt & A. Tsinober (Cambridge University Press, Cambridge) p157.
- Rust, D. M., & Kumar, A. 1996, *ApJ*, 464, L199
- Seehafer, N. 1990, *Solar Phys.*, 125, 219
- Seehafer, N. 1996, *Phys Rev E*, 53, 1283
- Woltjer, L., 1958, *Proc. Nat. Acad. Sci.*, 44, 80
- Zeldovich, Ya. B., Ruzmaikin, A. A., & Sokoloff, D. D. 1983, *Magnetic fields in astrophysics* (Gordon & Breach, New York)

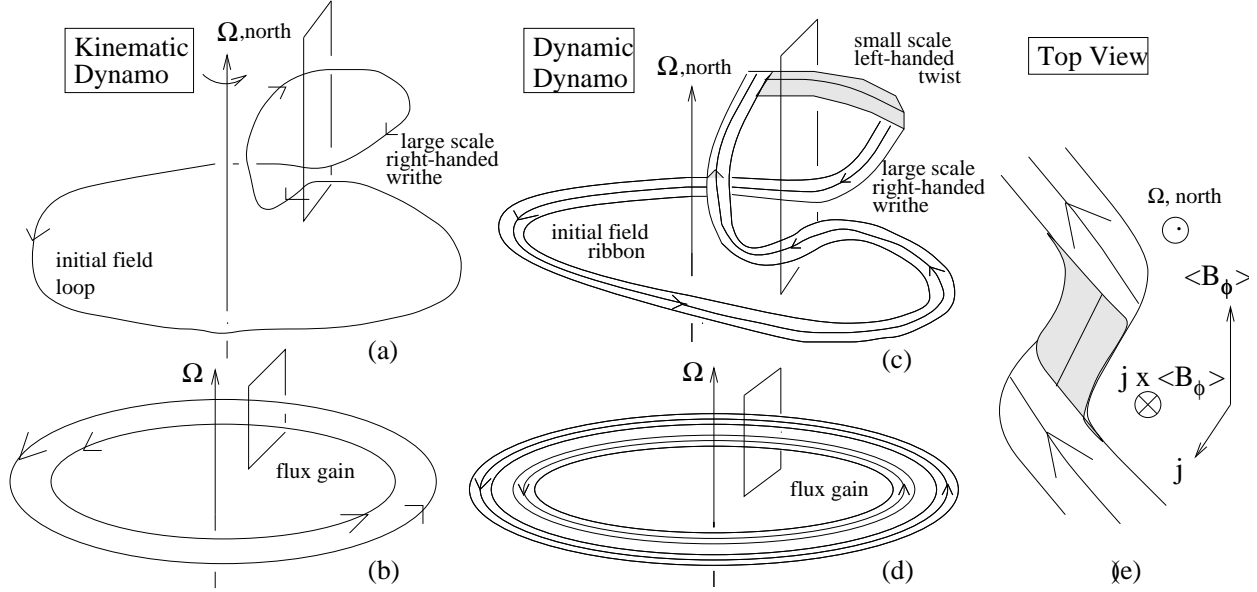


Fig. 1.— Schematic of *kinematic* helical $\alpha - \Omega$ dynamo in northern hemisphere is shown in (a) and (b), whilst the *dynamic* helical $\alpha - \Omega$ dynamo is shown by analogy in (c) and (d). Note that the mean field is represented as a line in (a) and (b) and as a ribbon in (c) and (d). (a) From an initial toroidal loop, the α effect induces a rising loop of right-handed writhe that gives a radial field component. (b) Differential rotation at the base of the loop shears the radial component, amplifying the toroidal component, and the ejection of the top part of loop (through coronal mass ejections) allow for a net flux gain through the rectangle. (c) Same as (a) but now with the field represented as a flux ribbon. This shows how the right-handed writhe of the large scale loop is accompanied by a left-handed twist along the ribbon, thus incorporating magnetic helicity conservation. (d) Same as (b) but with field represented as ribbon. (e) Top view of the combined twist and writhe that can be compared with observed coronal magnetic structures in active regions. Note the reverse S shape of the right-handed large scale twist in combination with the left-handed small scale twist along the ribbon. The backreaction force that resists the bending of the field ribbon is seen to result from the small scale twist. Note that diffusing the top part of the loops both allows for net flux generation in the rectangles of (a)-(d), and alleviates the backreaction that could otherwise quench the dynamo.

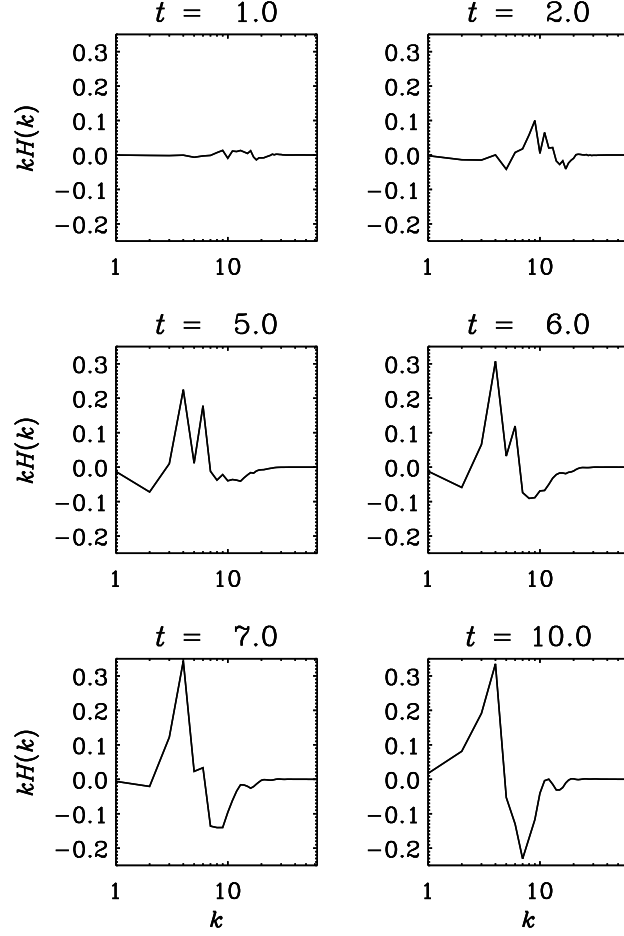


Fig. 2.— Magnetic helicity spectra from rising flux ribbon simulation (scaled by wavenumber k to give magnetic helicity per logarithmic interval) taken over the entire computational box. Positive (negative) helicity dominates at small (large) wavenumber.